Journal of Inorganic Biochemistry 104 (2010) 541–550

Contents lists available at ScienceDirect

Journal of Inorganic Biochemistry

journal homepage: www.elsevier.com/locate/jinorgbio

Transition metal ions and selenite modulate the methylation of arsenite by the recombinant human arsenic (+3 oxidation state) methyltransferase (hAS3MT)

Xiaoli Song [a], Zhirong Geng [a], Chengying Li [a], Xin Hu [b], Zhilin Wang [a,*]

[a] State Key Laboratory of Coordination Chemistry, School of Chemistry and Chemical Engineering, Nanjing University, Nanjing 210093, PR China
[b] Modern Analysis Center of Nanjing University, Nanjing 210093, PR China

ARTICLE INFO

Article history:
Received 29 April 2009
Received in revised form 8 January 2010
Accepted 11 January 2010
Available online 18 January 2010

Keywords:
Transition metal ions
Selenite
Human arsenic methyltransferase
Arsenite methylation

ABSTRACT

This report demonstrates that transition metal ions and selenite affect the arsenite methylation by the recombinant human arsenic (+3 oxidation state) methyltransferase (hAS3MT) in vitro. Co^{2+}, Mn^{2+}, and Zn^{2+} inhibited the arsenite methylation by hAS3MT in a concentration-dependent manner and the kinetics indicated Co^{2+} and Mn^{2+} to be mixed (competitive and non-competitive) inhibitors while Zn^{2+} to be a competitive inhibitor. However, only a high concentration of Fe^{2+} could restrain the methylation. UV–visible, CD and fluorescence spectroscopy were used to study the interactions between the metal ions above and hAS3MT. Further studies showed that neither superoxide anion nor hydrogen peroxide was involved in the transition metal ion or selenite inhibition of hAS3MT activity. The inhibition of arsenite methylating activity of hAS3MT by selenite was reversed by 2 mM DTT (dithiothreitol) but neither by cysteine nor by β-mercaptoethanol. Whereas, besides DTT, cysteine can also prevent the inhibition of hAS3MT activity by Co^{2+}, Mn^{2+}, and Zn^{2+}. Free Cys residues were involved in the interactions of transition metal ions or selenite with hAS3MT. It is proposed that the inhibitory effect of the ions (Co^{2+}, Mn^{2+}, and Zn^{2+}) or selenite on hAS3MT activity might be via the interactions of them with free Cys residues in hAS3MT to form inactive protein adducts.

1. Introduction

Arsenite and the methylated trivalent arsenic species which are metabolites of arsenate in humans and many other species [1–3] are multisite carcinogens [4–7]. Adverse health effects, resulting from chronic exposure to inorganic arsenic (iAs) in drinking water, such as increased risk of cancers and diseases on the circulatory, cardiovascular, and neurological system, have been well-studied. Methylation which is catalyzed by a SAM-dependent arsenic (+3 oxidation state) methyltransferase has been commonly regarded as the primary mechanism of detoxification of iAs in mammals [8]. However, the high affinity of methylated trivalent arsenic species for thiols, their uncoupling of mitochondrial oxidative phosphorylation, altering DNA repair and methylation patterns, changing growth factors, enhancing cell proliferation, and the bursts of reactive oxygen species (ROS) produced during the methylation may result in chronic metabolic alterations [9–13].

Arsenic and selenium are metalloids with similar chemical properties and metabolic conversions in vivo [14]. They act as metabolic antagonists. The original studies showed that both iAs^{3+} and iAs^{5+} protected laboratory animals against the toxicity of SeO_3^{2-}, selenocystine, and selenomethionine [15]. Trivalent arsenicals affect the selenoprotein synthesis in a Keratinocyte cell model [16]. On the other hand, the antagonist effects of selenium on metabolism of iAs^{3+} in organisms, cells, humans, rat liver cytosol, and even by a recombinant rat arsenic(+3) methyltransferase (AS3MT) and a recombinant human AS3MT have been studied [14,17–22]. The inhibition mechanisms perhaps include the antagonistic interactions between arsenic and selenium [23–25] and the direct interactions between selenium and AS3MT [19]. However, the inhibition mechanisms of selenium remain unclear. In addition, the combined effects of arsenic and antimony compounds have been studied in mammalian systems. IAs^{3+} methylation, in rat liver cytosol, is completely inhibited by $SbCl_3$ [26], and the chromosome mutagenicity induced by iAs is significantly suppressed by antimony(+3) in the micronucleus test with V79 cells [27]. The iAs^{3+} methylation is dramatically inhibited by antimony(+3) while the methylation of antimony is accelerated in the presence of iAs^{3+} by *Scopulariopsis brevicaulis* [28]. Some drugs, such as ampicillin, sodium molybdate, bromoethane sulfonate, monensin, and lasalocid also affected the iAs^{3+} methylation by bacteria in general, the sulfate reducing bacteria, and the methanoarchaea [29]. Meanwhile, many of other substances have been manifested to affect the metabolism of iAs^{3+}, such as Hg^{2+} [30].

Human depends on at least nine trace elements (iron, zinc, copper, manganese, iodine, chromium, selenium, molybdenum, and cobalt) for normal physical activities. They distribute in almost all of the tissues in human and serve a variety of functions including catalytic, structure, and regulatory activities. In organisms,

* Corresponding author. Tel.: +86 25 83592902; fax: +86 25 83593323.
E-mail address: wangzl@nju.edu.cn (Z. Wang).

0162-0134/$ - see front matter © 2010 Elsevier Inc. All rights reserved.
doi:10.1016/j.jinorgbio.2010.01.005

some of these trace elements undergo biomethylation as well [31]. Frankenberger and Arshad [32] reported the effects of trace elements on the iAs^{3+} methylation by a *Penicillium* sp. Kimpe studied the effects of metal ions on the iAs^{3+} methylation by rabbit liver cytosol [33]. The inhibition caused by these trace elements was speculated to be due to their effects on the enzyme [32]. However, there are no data of the influence of these trace elements on the iAs^{3+} methylation by purified enzyme at the present time.

Since iAs can cause liver cancer, hemolysis, marrow suppression, and blood vessels thickening, we chose the transition metals ($CoCl_2$, $ZnCl_2$, $MnCl_2$, $FeCl_2$) of these trace elements above, which show high concentration in the liver and marrow, skeletal muscle, bones, and blood, respectively to study their influence on the methylation of iAs^{3+} by hAS3MT in this report. As well, more studies were considered to probe the inhibition mechanism of selenite. Spectra (UV–visible (UV–vis), CD and fluorescence spectra) were used to study the interactions between these four transition metal ions and the hAS3MT. Co^{2+}, Mn^{2+}, and Zn^{2+} were the potent inhibitors of iAs^{3+} methylation by hAS3MT in different modes. The effects of Co^{2+}, Mn^{2+}, and Zn^{2+} on the structure and activity of hAS3MT were both in concentration-dependent manners. However, only a high concentration of Fe^{2+} could restrain the reaction. ROS were not involved in the inhibition of hAS3MT activity by both transition metal ions and selenite. The results demonstrate that transition metal ions and selenite affect the iAs^{3+} methylation by hAS3MT through their interactions with the enzyme in vitro.

2. Materials and methods

Caution: inorganic arsenic [34] and sodium selenite are classified as human carcinogens and should be handled accordingly.

2.1. Reagents

All chemicals were analytical grade or better. Expression host, *Escherichia coli* BL21 (DE3) pLysS was got from Novagen. Arsenicals were bought from J&K Chemical Ltd. Isopropyl β-D-thiogalactopyranoside (IPTG), 5,5′-dithiobis (2-nitrobenzoic acid) (DTNB), bovine serum albumin (BSA), S-adenosyl-methionine (SAM), dithiothreitol (DTT), cysteine, glutathione (GSH), β-mercaptoethanol (β-ME), and selenite were all bought from Sigma. All solutions were prepared using Milli-Q deionized water. The phosphate-buffered saline (PBS) was prepared from Na_2HPO_4 and NaH_2PO_4.

Stock solutions containing 1000 mg As L^{-1} each of the following species were prepared in Milli-Q deionized water: arsenite and arsenate prepared from $NaAsO_2$ (As^{3+}) and $Na_2HAsO_4{\cdot}7H_2O$ (As^{5+}), respectively; methylarsonate prepared from disodium methylarsonate (MMA); dimethylarsinate prepared from dimethylarsinic acid (DMA) (J&K Chemical Ltd.). All four of the stock solutions were stored at 4 °C in the dark. Working solutions of standards were prepared fresh daily from the stock solutions.

2.2. Preparation of hAS3MT

The cloning, expression, and purification of the recombinant hAS3MT were carried out as described previously [22]. Briefly, the hAS3MT gene was modified to eliminate the effect of the hairpin on the protein expression by site-directed mutagenesis. The modified gene was inserted into pET-32a vector to produce the expression plasmid. Expression host, *E. coli* BL21 (DE3) pLysS, was transformed by the ligated plasmid and the colonies were selected on standard ampicillin-containing agar plates and confirmed by restriction enzyme analysis. For expression, *E. coli* was cultured to the mid-log phase (OD_{600} 0.6–1.0) and then induced with 1 mM IPTG at 25 °C for 5 h. The cultured cells were harvested by centrifugation and sonicated on ice. After centrifugation, the cleared lysate was filtered through a 0.45 μm membrane and loaded onto a 2.5 mL Ni–NTA agarose column to purify the target protein. The purity of the hAS3MT was confirmed by SDS–PAGE and only a single band yielded. The purified enzyme was dialyzed three times against PBS (phosphate-buffered saline) (pH 7.0) for 24 h at 4 °C and protein concentration was determined by the Bradford assay based on a BSA standard curve.

2.3. UV–vis, CD and fluorescence spectroscopy

All spectra were recorded for the purified hAS3MT in 25 mM PBS (pH 7.0) at room temperature. UV–vis spectra were measured on a Perkin Elmer Lambda-35 spectrophotometer. Under the condition of the excitation wavelength of hAS3MT, 290 nm, the fluorescence emission spectra were recorded on a 48,000 DSCF time-resolved fluorescence spectrometer (SLM Co., USA). CD (195–250 nm) spectra were recorded on a JASCO-J810 spectropolarimeter (Jasco Co., Japan) with 1 mm slit width and 10 mm light length at the scanning rate, 50 nm/min. The spectra were the average of three readings and the secondary structure parameters of hAS3MT were computed using Yang. jwr software [35].

The spectra titrations of hAS3MT in PBS buffer were performed by using a fixed protein concentration to which increments of the Co^{2+}, Zn^{2+}, Mn^{2+}, and Fe^{2+} fresh solutions were added, respectively. Protein solution employed was 4 μM in concentration and the ratio of $[M^{2+}]$/[protein] was ranged from 0 to 2.5. Protein–M^{2+} solutions were allowed to incubate for 10 min before the spectra were recorded.

2.4. Methylation assay in the presence of transition metal ions

The reaction mixtures (100 μL) contained 25 mM PBS (pH 7.0), 11 μg hAS3MT, 7 mM GSH, 1 mM SAM, and varying amounts of iAs^{3+}. PBS or fresh solutions of transition metal chloride and selenite were added to reaction mixtures to reach a final volume of 100 μL. To determine the effects of transition metal ions on the activity of hAS3MT, the methylation of 1 μM iAs^{3+} was examined by hAS3MT in the absence and presence of 0.05–100 μM (concentrations were arbitrarily chosen with the literature average values for packed blood cells as a guideline [36]) corresponding metal ions. Reaction mixtures were incubated in capped tubes at 37 °C for the desired times. Because trivalent arsenicals are known to bind to proteins [37], the incubated samples were treated with H_2O_2 at a final concentration of 3% to convert all arsenic metabolites to pentavalency to release the trivalent arsenic metabolites from enzyme before analysis. Then the reactions were quenched by boiling the samples for 5 min and the denatured proteins were removed by centrifugation. A 20 μL aliquot of each sample was separated on an anion-exchange column (PRP-X100 250 mm × 4.6 mm i.d., 5 μm, Hamilton) using 15 mM $[NH_4]_2HPO_4$, adjusted to pH 6.0 with H_3PO_4, as the mobile phase with a flow rate of 1.2 mL/min [38–40]. Arsenicals of the separated species were detected by an Elan 9000 ICP-MS. The amounts of arsenic species were calculated from the working curves prepared using 5, 10, 20, 40, 80, and 160 μg As L^{-1} of standard arsenic species with the Chromera software. Methylation rates were calculated as mole equivalents of methyl groups transferred from SAM to iAs^{3+} (i.e., 1 pmol CH_3 per 1 pmol MMA or 2 pmol CH_3 per 1 pmol DMA) [18].

2.5. Titration of free thiol groups in the solutions of hAS3MT–M^{2+}/SeO_3^{2-}

The concentration of free thiol groups in the solutions of hAS3MT–M^{2+}/SeO_3^{2-} was determined by the method of Ellman [41]. The solutions of hAS3MT–M^{2+}/SeO_3^{2-} (enzyme-inhibitors)

([M^{2+} or SeO_3^{2-}]/[protein] = 1, 2, 4), containing 3.6×10^{-4} μmol enzyme, were incubated at 37 °C for 2 h in cuvets. After the incubation, 10 μL DTNB (0.01 M in 0.05 M PBS, pH 7.0) was added and then Tris–HCl buffer (0.05 M, pH 8.0) was appended to the reaction mixtures to reach a final volume 1.0 mL. The reaction was carried out at 25 °C for 30 min, and the release of 2-nitro-5-mercaptobenzoic acid was followed at 412 nm, using Perkin Elmer Lambda-35 spectrophotometer. Each sample had a control in which only corresponding concentration of M^{2+} or SeO_3^{2-} was added. The concentration of free thiol groups was calculated with the working curves prepared using 0.5, 1, 2.5, 5, 10, and 20 μM of cysteine.

3. Results

3.1. Effects of Co^{2+}, Mn^{2+}, Zn^{2+}, and Fe^{2+} on iAs^{3+} methylation by hAS3MT

The arsenic metabolites were separated and detected by HPLC–ICP-MS (inductively coupled plasma mass spectrometry) (Fig. 1) and the amounts were calculated from the working curves prepared using standard arsenic species with the Chromera software. Co^{2+}, Mn^{2+}, and Zn^{2+} all exhibited a concentration-dependent manner in the inhibition of iAs^{3+} methylation by hAS3MT. But only a high concentration of Fe^{2+} could suppress the reaction (Fig. 2). Kinetic analysis characterized the inhibition of hAS3MT activity by Co^{2+}, Mn^{2+}, and Zn^{2+} over a range of iAs^{3+} concentrations from 1 to 5 μM. Double reciprocal (1/V vs 1/[iAs^{3+}]) plots show both Co^{2+} and Mn^{2+} to be mixed (competitive and non-competitive) inhibitors of iAs^{3+} methylation by hAS3MT (Fig. 3A and B), while Zn^{2+} to be a competitive inhibitor (Fig. 3C). SeO_3^{2-} has been shown to be a non-competitive inhibitor of the methylation of iAs^{3+} by hAS3MT [22]. The K_i values of 1.70 μM for Co^{2+}, 3.98 μM for Mn^{2+}, and 0.49 μM for Zn^{2+} were calculated from the replots of the slopes vs the concentrations of the inhibitors (Fig. 3, insets). A 24 h dialysis against 25 mM PBS (pH 7.0) at 4 °C reversed the inhibition of hAS3MT activity by Co^{2+} or Mn^{2+} up to 80% while that by Zn^{2+} or SeO_3^{2-} was almost totally reversed (Fig. 4). CD spectra monitored the secondary structures of hAS3MT–M^{2+}/SeO_3^{2-} enzyme after a 24 h dialysis at 4 °C (Table 1). The content of each secondary structure of hAS3MT–Zn^{2+}/SeO_3^{2-} enzyme is consistent with that of hAS3MT (29.0% α-helix, 23.9% β-pleated sheet, 17.9% β-turn, and 29.2% random coil) [22,42] after a 24 h dialysis at 4 °C. However, the conformation of hAS3MT–Co^{2+}/Mn^{2+} enzyme can not be totally reversed, with the content of α-helix increased while that of β-pleated sheet decreased. ICP-MS analysis showed that there was no metal or selenite left in the enzyme–M^{2+}/SeO_3^{2-} solutions after the dialysis.

3.2. Interactions of Co^{2+}, Mn^{2+}, Zn^{2+}, and Fe^{2+} with hAS3MT

The interactions of these four transition metal ions with hAS3MT were determined, respectively by UV–vis, CD and fluorescence spectra. Fig. 5 shows a well-behaved titration of hAS3MT with Co^{2+}, Mn^{2+}, and Zn^{2+} in the UV–vis spectra. Co^{2+} and Mn^{2+} yielded hypochromism while Zn^{2+} showed hyperchromism. The CD spectra for hAS3MT in the absence and presence of increasing concentrations of Co^{2+}, Mn^{2+}, and Zn^{2+} are displayed in Fig. 6. When Co^{2+}, Mn^{2+}, and Zn^{2+} were added, respectively, the intensities of the CD spectra decreased gradually. The content of α-helix decreased while that of β-pleated sheet increased (the total content of α + β had little change) in the secondary structure of hAS3MT when Co^{2+} or Mn^{2+} was added. The titration of Zn^{2+} also

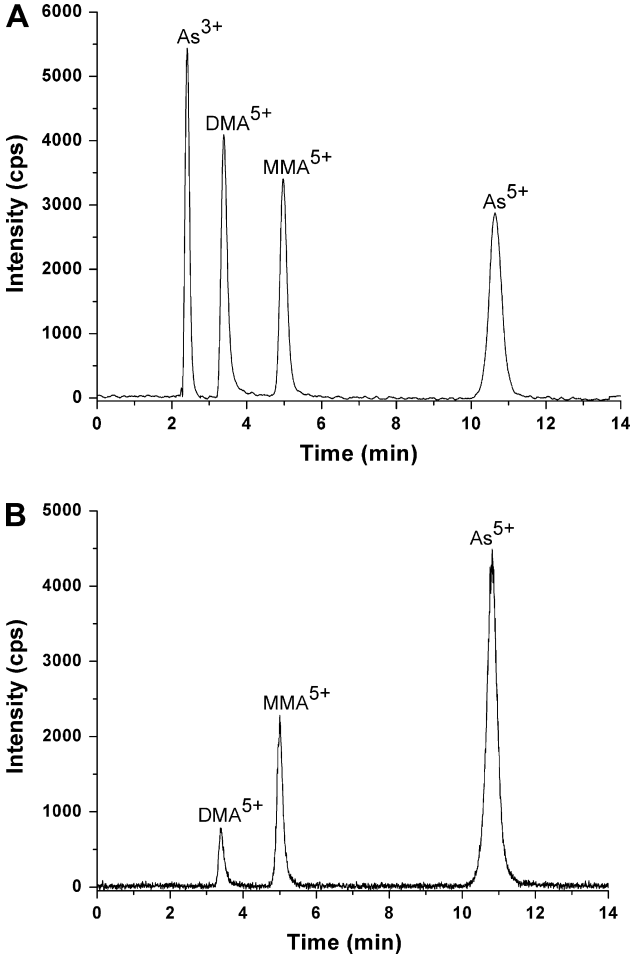

Fig. 1. Elution profiles of arsenicals on a PRP-X100 column by HPLC–ICP-MS. (A) A 20 μL of authentic arsenicals (30 ppb) such as inorganic arsenic (As^{3+}), dimethylarsinic acid (DMA^{5+}), monomethylarsonic acid (MMA^{5+}), and inorganic arsenic (As^{5+}). (B) A 20 μL of arsenicals from an enzymatic assay mixture. The reaction mixture (100 μL), containing 11 μg hAS3MT, 1 mM SAM, 7 mM GSH, 1 μM iAs^{3+}, in 25 mM PBS (pH 7.0), was incubated at 37 °C for 1.5 h. The sample was treated with H_2O_2 before analysis.

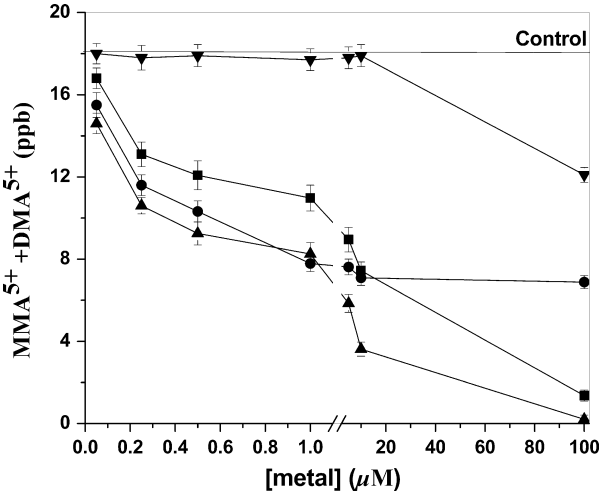

Fig. 2. Modulation of iAs^{3+}-methylation activity of hAS3MT by Co^{2+}, Mn^{2+}, Zn^{2+}, and Fe^{2+}. Reaction mixtures (100 μL), containing 11 μg hAS3MT, 1 mM SAM, 7 mM GSH, 1 μM iAs^{3+}, and varying amounts of M^{2+} (0.05–100 μM) in 25 mM PBS (pH 7.0), were incubated at 37 °C for 2 h. Plots for Co^{2+} (■), Mn^{2+} (●), Zn^{2+} (▲), and Fe^{2+} (▼). Control, reaction mixture incubated without metal ions. Values are the means ± SD of four separate experiments.

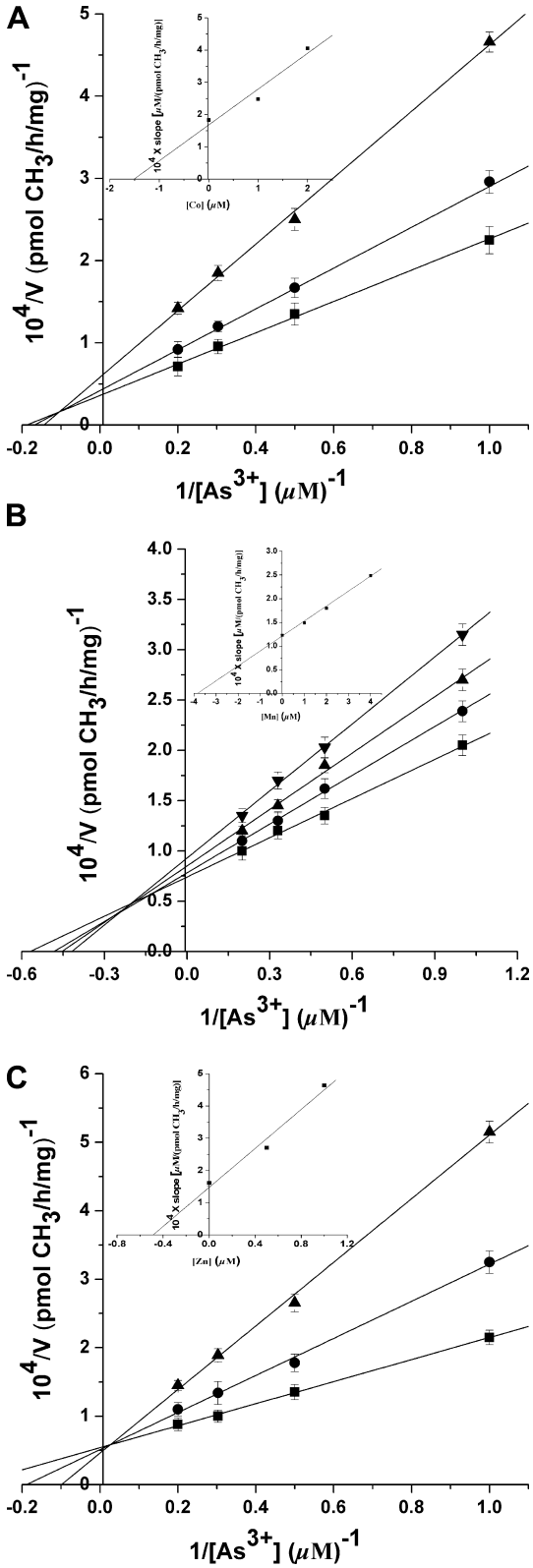

Fig. 3. Double reciprocal plots for the inhibition of iAs^{3+} methylation by Co^{2+}, Mn^{2+}, and Zn^{2+}. The reaction mixtures (100 μL), containing 11 μg hAS3MT, 1 mM SAM, 7 mM GSH, 25 mM PBS (pH 7.0) with iAs^{3+} indicated were incubated at 37 °C for 1.5 h. (A) Co^{2+}, plots for 0 μM (■), 1 μM (●), and 2 μM (▲) Co^{2+}. (B) Mn^{2+}, plots for 0 μM (■), 1 μM (●), 2 μM (▲), and 4 μM (▼) Mn^{2+}. (C) Zn^{2+}, plots for 0 μM (■), 0.5 μM (●), and 1 μM (▲) Zn^{2+}. Replots of slopes vs concentrations of inhibitors are shown in the insets. Values are the means ± SD of four separate experiments.

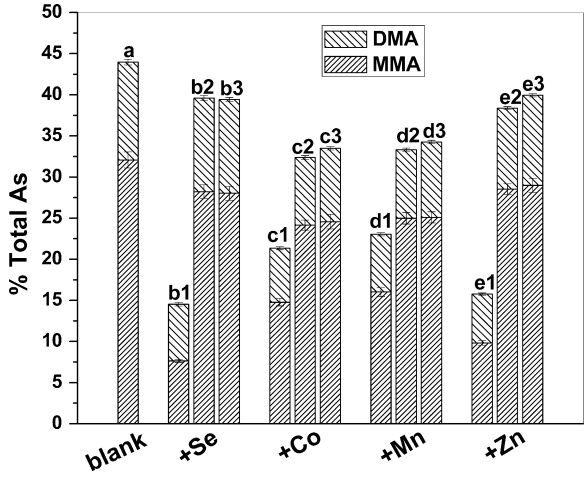

Fig. 4. Effects of dialysis on the inhibition of hAS3MT by M^{2+} or SeO_3^{2-}. (a) Control, The reaction mixture (100 μL), containing 11 μg hAS3MT, 1 mM SAM, 7 mM GSH, 1 μM iAs^{3+}, and 25 mM PBS (pH 7.0) was incubated at 37 °C for 1.5 h. (b1) SeO_3^{2-} to 2 μM was added to 500 μL reaction mixture as (a) and was incubated at 37 °C for 1.5 h, 100 μL was taken out for analysis. (b2) The rest of (b1) was dialyzed three times against 25 mM PBS (pH 7.0) at 4 °C for 24 h and the protein concentration in the solution was determined by the Bradford assay based on a BSA standard curve. Then the reaction mixture containing the same content of each component as (a) was incubated at 37 °C for 1.5 h. (b3) EDTA to 10 μM was added to 100 μL of (b2) and was incubated at 37 °C for 1.5 h. (c1–c3) Co^{2+} to 2 μM was added. The methods were the same as that of (b1–b3), respectively. (d1–d3) Mn^{2+} to 2 μM was added. The methods were the same as that of (b1–b3), respectively. (e1–e3) Zn^{2+} to 1 μM was added. The methods were the same as that of (b1–b3), respectively. Values are the means ± SD of four separate experiments.

Table 1
Secondary structures of hAS3MT–M^{2+}/SeO_3^{2-} enzyme after 24 h dialysis at 4 °C.[a]

	α%	β%	Turn%	Random%
hAS3MT[22]	29.0 ± 2.2	23.9 ± 1.9	17.9 ± 1.7	29.2 ± 1.4
E-Se[b]	28.4 ± 1.8	23.5 ± 1.6	19.2 ± 2.6	28.9 ± 1.8
E-Co[b]	36.1 ± 1.3	16.1 ± 1.5	24.2 ± 1.1	20.6 ± 2.7
E-Mn[b]	35.6 ± 2.4	16.2 ± 1.1	27.5 ± 3.0	20.7 ± 1.6
E-Zn[b]	25.8 ± 2.1	28.3 ± 2.5	19.4 ± 3.1	26.5 ± 2.9

[a] Values are the means ± SD of four separate experiments.
[b] hAS3MT in the dialysis solutions described in Fig. 4 (b2–e2).

gave rise to the decrease of α-helix and increase of β-pleated sheet but the total content of α + β increased dramatically. The varieties in the fluorescence spectra of hAS3MT with the increasing amounts of Co^{2+}, Mn^{2+}, and Zn^{2+} are given in Fig. 7. Under the excitation wavelength of 290 nm, hAS3MT had maximal fluorescence at about 348 nm. The fluorescence intensities decreased with about 4 nm red shift in the emission band when Co^{2+}, Mn^{2+}, and Zn^{2+} was added, respectively. Meanwhile, another peak appeared at about 408 nm when Co^{2+} or Mn^{2+} was added. Differently, Fe^{2+} had little effect on these three spectra of hAS3MT in the investigated [Fe^{2+}]/[protein] range from 0 to 5 (data not shown).

3.3. Concentration of free thiol groups in the solutions of hAS3MT–M^{2+}/SeO_3^{2-}

The thiol contents of the solutions of hAS3MT–M^{2+}/SeO_3^{2-} are listed in Table 2. The content of free thiol groups in hAS3MT is 4.39 (thiol group/mol of enzyme). With the ratio of [M^{2+} or SeO_3^{2-}]/[protein] increasing, the thiol contents of the solutions decreased. Thus, the interactions of M^{2+} or SeO_3^{2-} with hAS3MT involved free Cys residues.

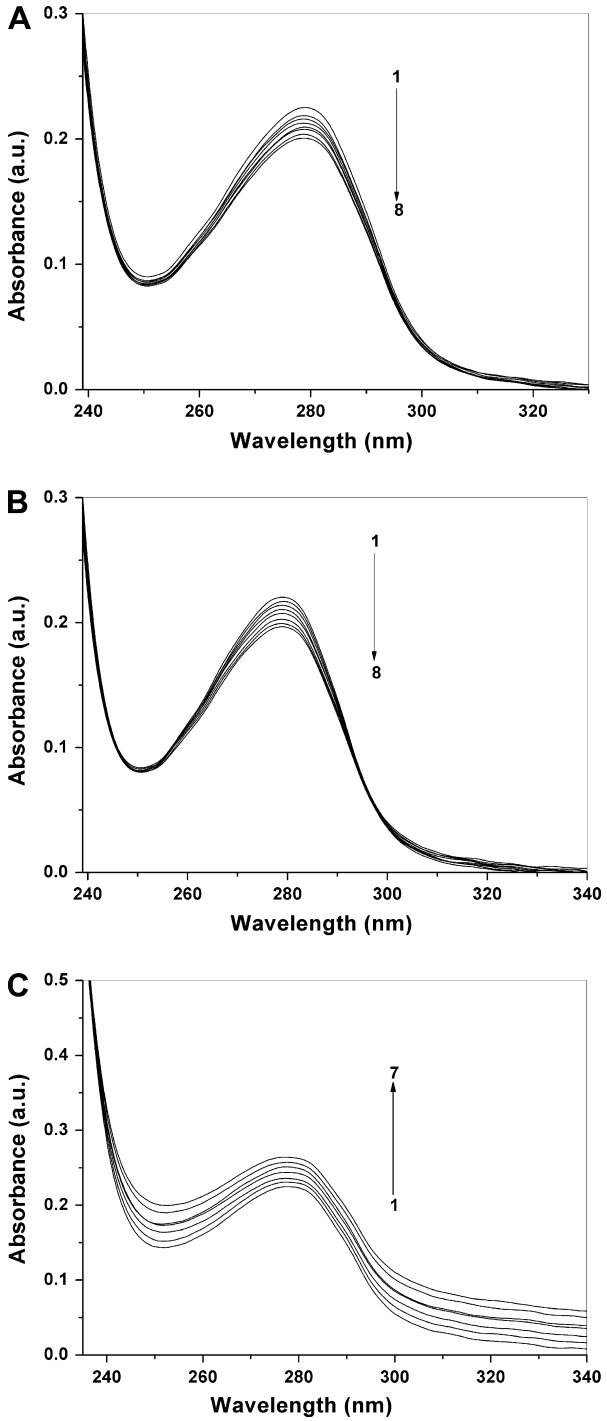

Fig. 5. UV–vis spectra of hAS3MT in the absence and presence of increasing amounts of M^{2+} in 25 mM PBS (pH 7.0) at room temperature. The concentration of hAS3MT was 4 μM. (A) Co^{2+}, the $[Co^{2+}]$/[hAS3MT] rates were 0, 0.1, 0.3, 0.5, 0.8, 1.0, 1.2, 1.5. (B) Mn^{2+}, the $[Mn^{2+}]$/[hAS3MT] rates were 0, 0.1, 0.3, 0.5, 0.8, 1.0, 1.2, 1.5. (C) Zn^{2+}, the $[Zn^{2+}]$/[hAS3MT] rates were 0, 0.1, 0.3, 0.6, 1.0, 1.5, 2.0. Arrows indicate the change in absorbance upon increasing M^{2+} concentrations.

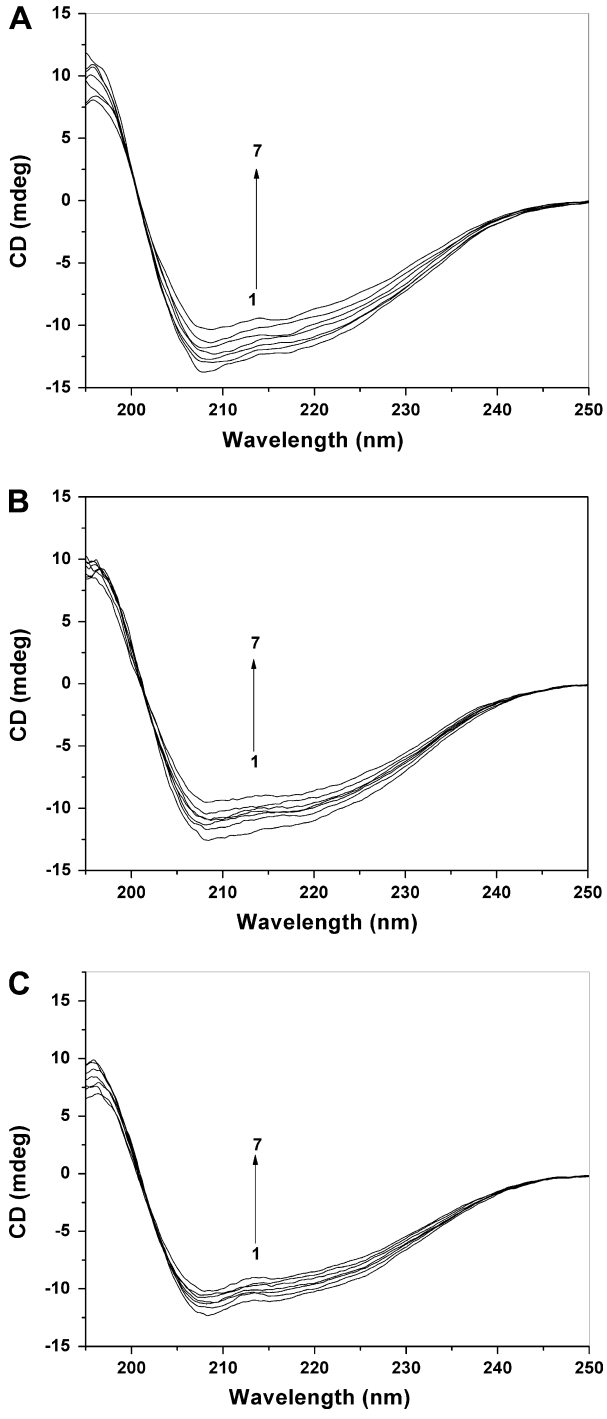

Fig. 6. CD spectra of hAS3MT in the absence and presence of increasing amounts of M^{2+} in 25 mM PBS (pH 7.0) at room temperature. The concentration of hAS3MT was 4 μM. (A) Co^{2+}, the $[Co^{2+}]$/[hAS3MT] rates were 0, 0.25, 0.5, 0.75, 1.25, 1.5, 2.0. (B) Mn^{2+}, the $[Mn^{2+}]$/[hAS3MT] rates were 0, 0.25, 0.75, 1, 1.5, 2.0, 2.5. (C) Zn^{2+}, the $[Zn^{2+}]$/[hAS3MT] rates were 0, 0.2, 0.4, 0.8, 1.2, 1.8, 2.0. Arrows indicate the change in CD spectra upon increasing M^{2+} concentrations.

3.4. Effects of deoxidant on the inhibition of hAS3MT activity by [1] Zn^{2+}, Co^{2+}, Mn^{2+}, and SeO_3^{2-}

Hydrogen selenide is one of the products in the reaction of selenite with GSH and it can be converted to Se^0 with the production of superoxide anion [43]. So it was pertinent to determine the possible involvement of superoxide anion (O_2^-) and H_2O_2 in the selenite inhibition of hAS3MT activity. ROS such as O_2^-, $OH^{\cdot}$, and singlet dioxygen, can be cleared out by L-ascorbic. Then inhibition assays by SeO_3^{2-} were carried out in the presence of sodium ascorbate or catalase. Sodium ascorbate, 2 or 4 mM, did not prevent the inhibition of hAS3MT activity, neither did catalase (Fig. 8). SeO_3^{2-}

[1] Fe^{2+} *affected the iAs3+ methylation* only in a very high concentration. Thus, we did not test the following experiments.

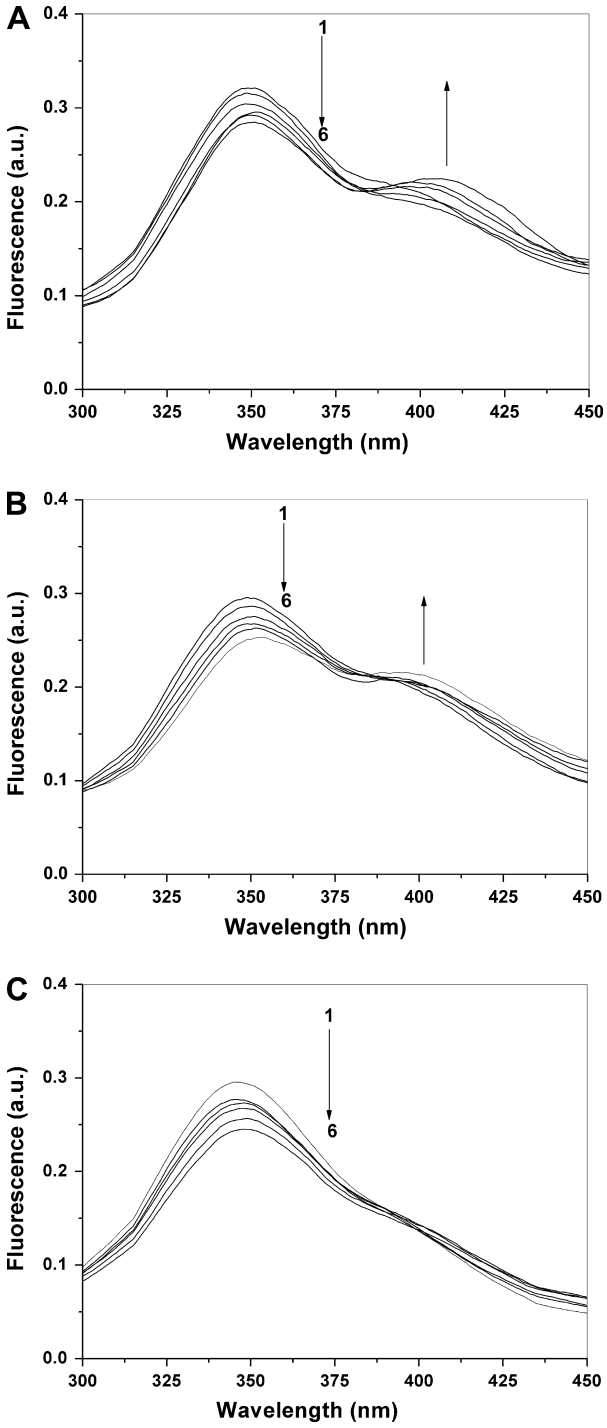

Fig. 7. Fluorescence emission spectra of hAS3MT in the absence and presence of increasing amounts of M^{2+} in 25 mM PBS (pH 7.0) at room temperature. The concentration of hAS3MT was 4 μM. (A) Co^{2+}, the $[Co^{2+}]/[hAS3MT]$ rates were 0, 0.1, 0.2, 0.5, 0.8, 1.0. (B) Mn^{2+}, the $[Mn^{2+}]/[hAS3MT]$ rates were 0, 0.1, 0.2, 0.5, 0.8, 1.0. (C) Zn^{2+}, the $[Zn^{2+}]/[hAS3MT]$ rates were 0, 0.1, 0.2, 0.3, 0.5, 0.8. Arrows indicate the change in fluorescence intensity upon increasing M^{2+} concentrations. λ (excitation) and λ (emission) were 290 nm and 348 nm, respectively.

did not inhibit the activity of catalase in reducing hydrogen peroxide [43]. Therefore, ROS were not involved in the SeO_3^{2-} inhibition of hAS3MT activity. Corresponding inhibition experiments by Co^{2+}, Mn^{2+}, or Zn^{2+} were investigated in the presence of sodium ascorbate and it did not prevent the inhibition as well (data not shown).

Table 2
Concentration of free thiol groups of hAS3MT in the presence of M^{2+} or SeO_3^{2-} [a].

	Thiol group/mol of enzyme		
	[c]1:1	2:1	4:1
E-Se[b]	3.50 ± 0.30	2.75 ± 0.26	2.20 ± 0.11
E-Fe[b]	2.85 ± 0.40	2.48 ± 0.19	1.96 ± 0.39
E-Co[b]	3.80 ± 0.25	3.33 ± 0.30	1.15 ± 0.23
E-Mn[b]	3.60 ± 0.16	2.88 ± 0.18	1.36 ± 0.19
E-Zn[b]	2.83 ± 0.35	2.25 ± 0.23	0.63 ± 0.17

[a] Values are the means ± SD of four separate experiments.
[b] hAS3MT–M^{2+}/SeO_3^{2-} enzyme.
[c] The ratio of $[M^{2+}/SeO_3^{2-}]/[hAS3MT]$.

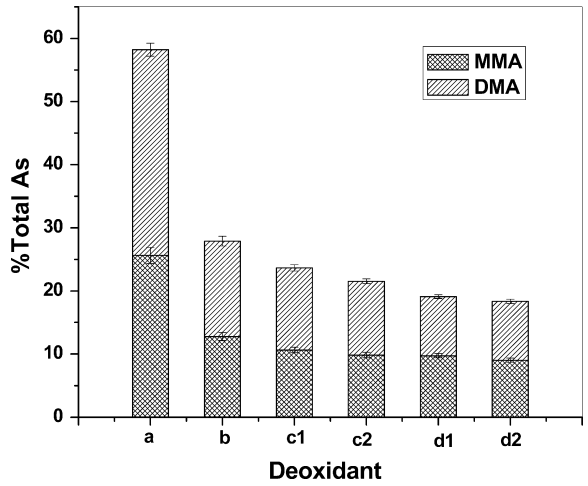

Fig. 8. L-Ascorbic acid and catalase did not prevent SeO_3^{2-} inhibition of hAS3MT activity. The reaction mixture (100 μL) containing 11 μg hAS3MT, 1 mM SAM, 7 mM GSH, 1 μM iAs^{3+}, and 25 mM PBS (pH 7.0) was incubated at 37 °C for 2 h. (a) No SeO_3^{2-}, no ascorbate, no catalase. (b) Pluse 1.5 μM SeO_3^{2-}. (c1) Pluse 1.5 μM SeO_3^{2-}, pluse 2 mM ascorbate. (c2) Pluse 1.5 μM SeO_3^{2-}, pluse 4 mM ascorbate. (d1) Pluse 1.5 μM SeO_3^{2-}, pluse 2 μg catalase. (d2) Pluse 1.5 μM SeO_3^{2-}, pluse 4 μg catalase. Values are the means ± SD of four separate experiments.

3.5. Effects of reductant on the inhibition of hAS3MT activity by Co^{2+}, Mn^{2+}, Zn^{2+}, and SeO_3^{2-}

The inhibition of hAS3MT activity by SeO_3^{2-} was substantially reversed by incubation with 2 mM DTT for an additional 1 h. Nevertheless, inhibition by SeO_3^{2-} was not prevented by 10 mM cysteine or 10 mM β-ME (Fig. 9A). For the inhibition by Co^{2+}, Mn^{2+}, and Zn^{2+}, 10 mM cysteine or 2 mM DTT but not 10 mM β-ME reversed it substantially (Fig. 9B).

4. Discussion

Arsenite and arsenate are important worldwide environmental toxicants of both natural and anthropogenic sources [44,45]. It is generally accepted that inorganic arsenicals are methylated by arsenic(+3) methyltransferase (AS3MT) through repetitive reduction and oxidative methylation to form pentavalent methylated arsenicals, such as monomethylarsonic acid (MMA^V) and dimethylarsinic acid (DMA^V), which are excreted mainly in urine [46–48]. Various reports have implicated different steps in this pathway as being susceptible to inhibition by selenite, antimonite, and other substances [14,15,26–33]. However, there are no data about the influence of metal ions on the iAs^{3+} methylation by purified enzyme at the present time and neither the inhibition mechanisms.

Therefore, we chose some transition metals (Co, Zn, Mn, Fe) showing high concentration in the organs that would be damaged

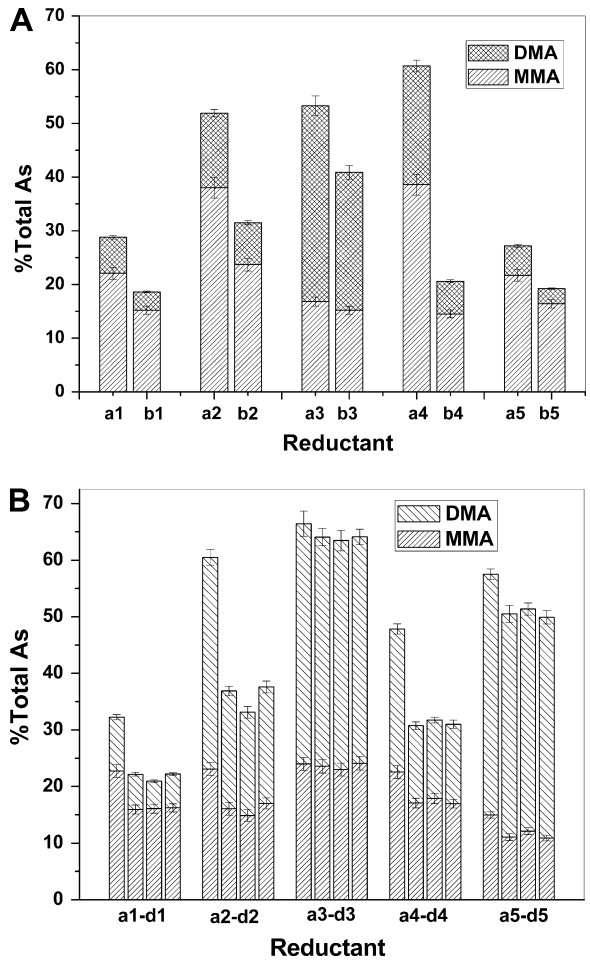

Fig. 9. (A) Effects of reductants on the inhibition of hAS3MT activity by SeO_3^{2-}. (a1) Four tubes of reaction mixtures (11 μg hAS3MT, 1 mM SAM, 7 mM GSH, 1 μM iAs^{3+}, and 25 mM PBS (pH 7.0)), 500 μL per tube, were incubated for 1 h at which time 100 μL was removed from each tube to determine hAS3MT activity. (b1) As in panel (a1) but in the presence of 1.5 μM SeO_3^{2-}. (a2–b2) A 100 μL amount of (a1), (b1) was incubated for an additional 1 h. (a3–b3) DTT to 2 mM was added to a 100 μL amount of (a1), (b1), respectively and incubated for an additional 1 h. (a4–b4) Cysteine to 10 mM was added to a 100 μL amount of (a1), (b1), respectively and incubated for an additional 1 h. (a5–b5) β-ME to 10 mM was added to a 100 μL amount of (a1), (b1), respectively and incubated for an additional 1 h. (B) Effects of reductants on the inhibition of hAS3MT by M^{2+}. (a1) Four tubes of reaction mixtures (11 μg hAS3MT, 1 mM SAM, 7 mM GSH, 1 μM iAs^{3+}, and 25 mM PBS (pH 7.0)), 500 μL per tube, were incubated for 1 h at which time 100 μL was removed from each tube to determine hAS3MT activity. (b1–d1) As in panel (a1) but in the presence of 1 μM Co^{2+}, 0.5 μM Zn^{2+}, 2 μM Mn^{2+}, respectively. (a2–d2) A 100 μL amount of (a1–d1) was incubated for an additional 1 h. (a3–d3) Cysteine to 10 mM was added to a 100 μL amount of (a1–d1) and incubated for an additional 1 h. (a4–d4) β-ME to 10 mM was added to a 100 μL amount of (a1–d1) and incubated for an additional 1 h. (a5–d5) DTT to 2 mM was added to a 100 μL amount of (a1–d1) and incubated for an additional 1 h. Values are the means ± SD of four separate experiments.

by metabolizing or transmitting arsenic to study their influence on the methylation of iAs^{3+} by hAS3MT. Meanwhile, further studies were considered to study the interaction modes of selenite and metal ions with hAS3MT to probe the inhibition mechanism. Kinetic analysis showed both Co^{2+} and Mn^{2+} to be mixed (competitive and non-competitive) inhibitors of iAs^{3+} methylation by hAS3MT and Zn^{2+} seemed to be a competitive inhibitor. However, only a high concentration of Fe^{2+} could restrain the methylation. SeO_3^{2-} has been shown to be a non-competitive inhibitor of the methylation of iAs^{3+} by hAS3MT in our previous report [22].

The inhibition of enzyme activity by selenite usually has been stated to attribute to its affinity for sulfhydryl groups of the enzymes [19,22]. This interaction between selenite and the enzymes possibly alters the conformation of the proteins and makes them inactive. Accordingly, since transition metal ions are prone to coordinate with atoms which are rich in electrons, we hypothesized that transition metal ions might modify the structure of hAS3MT due to their coordination with some amino acid residues of the enzyme. So in our experiments, we monitored the interactions between transition metal ions and hAS3MT by UV–vis, CD and fluorescence spectra. The intrinsic UV–vis absorbance peak of hAS3MT at 278 nm is mainly caused by Trp and Tyr in hAS3MT. The titration of transition metal ions induced large spectral perturbations in the specific absorption peak. Co^{2+} and Mn^{2+} yielded hypochromism while Zn^{2+} showed hyperchromism. These spectral varieties displayed the change of the microenvironment of aromatic chromophores owing to the interactions between hAS3MT and the transition metal ions. The changes in the conformation of hAS3MT caused by Zn^{2+} made the chromogenic residues exposed while that caused by Co^{2+} and Mn^{2+} made the chromogenic residues embedded into the interior of the protein, which gave rise to hyperchromism and hypochromism, respectively. These varieties also indicated the way by which Zn^{2+} combined with hAS3MT was different from that for Co^{2+} and Mn^{2+}. Protein secondary structure can be probed by CD spectroscopy in the far UV [34,49,50]. At the far UV range, the chromophores are the peptide bonds, and signal arises when they are located in a regular, folded environment. Alpha-helix, β-pleated sheet, and random coil structures each causes a characteristic shape and magnitude of CD spectrum [50]. The CD spectra of hAS3MT showed a positive peak at 195 nm and two negative peaks at 208 nm and 222 nm, respectively. It was analyzed to have the secondary structures of 29.0% α-helix, 23.9% β-pleated sheet, 17.9% β-turn, and 29.2% random coil [22]. CD is remarkably sensitive to protein secondary structure and can be applied to protein in solution. Thus, CD can be used to follow changes of protein secondary structure in solvent composition or that in biomolecular interactions [51]. When Co^{2+}, Mn^{2+}, or Zn^{2+} was added, the intensities of the CD spectra of hAS3MT decreased gradually. The content of each secondary structure was changed. These may attribute to the hAS3MT–M^{2+} interactions which made the peptide bonds in a disorderly and unfolded environment. Proteins contain three aromatic amino acid residues (Trp, Tyr, Phe) which may offer intrinsic fluorescent probes of protein conformation, dynamics, and intermolecular interactions [52]. Of these three aromatic amino acids, Trp is the most popular probe. It has the strongest fluorescence and highest quantum yield and is highly sensitive to environment, making it an ideal choice for monitoring protein conformation changes and interactions with other molecules. Trp fluorescence is uniquely sensitive to collisional quenching, either by externally added quenchers or by nearby protonated acidic groups in the protein [52,53]. The wavelength of the emission maximum is a good indication of the environment of the fluorophore [54]. The hAS3MT had a maximal fluorescence at about 348 nm at the excitation wavelength of 290 nm. This result demonstrated that Trp residues were exposed to water, not buried into the inside of hAS3MT. There are three Trp residues (at positions 73, 203, and 213) in the hAS3MT, each of which is located beside protonated acidic groups (Asp76, Glu205 and Glu215) and Cys residues (Cys72, Cys206 and Cys226). The hAS3MT fluorescence was quenched gradually with a red shift by the increasing concentrations of transition metal ions. Because Trp fluorescence is sensitive to environment and collisional quenching, we speculate that transition metal ions might change the microenvironment around Trp residues owing to their coordination with some electron-rich group residues or Cys residues beside the Trp residues in hAS3MT and then Trp fluorescence might be quenched by neighbouring protonated acidic groups. Also, our results show that the side chains of corresponding Trp residues, protonated acidic groups,

and Cys residues are in close proximity to each other [55]. Another peak appeared at about 408 nm when Co^{2+} or Mn^{2+} but not Zn^{2+} was added. This indicate that the way by which Co^{2+} and Mn^{2+} act on hAS3MT is different from that by Zn^{2+} and these results are consistent with our data from CD and UV–vis. In addition, the protein-metal adducts may be confirmed according to the new peak at 408 nm in the fluorescence spectra. Our results indicated that Co^{2+}, Mn^{2+}, and Zn^{2+} could modify the structure of hAS3MT through their interactions with the enzyme. The differences in the inhibition modes and the interaction modes with the hAS3MT between Zn^{2+} and Co^{2+}/Mn^{2+} appear to be due to the differences in the electronic structure of Zn^{2+} and Co^{2+}/Mn^{2+}, that is diamagnetism of the former and paramagnetism of the latter.

Selenite requires six electrons for the bioreductive activation of one selenium(+4) atom to selenodisulfide (RS-Se-SR) prior to eliciting its therapeutic or pro-oxidant activity. The subsequent formation of selenopersulfide (RS-SeH) and selenide (H_2–Se) is a critical step in the utilization of selenium [56,57]. The pro-oxidant catalytic activity of selenite is considered to be owing to the reaction of hydrogen selenide with oxygen to produce O_2^-, H_2O_2, other cascading oxyradicals, and elemental selenium [58]. In order to determine whether the inhibition of hAS3MT activity by SeO_3^{2-} involved these products, our experiments were performed in the presence of sodium ascorbate, a scavenger of superoxide, and catalase. But neither sodium ascorbate nor catalase blocked the selenite inhibition of hAS3MT activity (Fig. 8). Corresponding inhibition experiments by Co^{2+}, Mn^{2+}, or Zn^{2+} were also investigated in the presence of sodium ascorbate. As well, sodium ascorbate did not prevent the inhibition (data not shown). Thus, it was unlikely that O_2^- or H_2O_2 was involved in the selenite and transition metal ion inhibition of hAS3MT activity.

DTNB has been extensively used for probing free thiol groups in proteins [41]. Then we used this reagent to study whether free Cys residues were involved in the interaction of M^{2+} or SeO_3^{2-} with hAS3MT since free thiol is only contained in free Cys residues in proteins. With the ratio of [M^{2+} or SeO_3^{2-}]/[protein] increasing, the thiol contents of the solutions decreased. Thus, we speculate that the interaction of M^{2+} or SeO_3^{2-} with hAS3MT involves free Cys residues.

Integrating the results obtained from the above assays, we considered that the inhibition of enzyme activity by transition metal ions is due to the modification on the structure of hAS3MT by the interactions with some amino acid residues (active sites or non-active sites) of the enzyme. Fomenko reported that Cys157 and Cys207 were the active sites of the recombinant mouse AS3MT [59]. Correspondingly, Cys156 and Cys206 were confirmed to be the active sites of hAS3MT by protein sequence align analysis and site-directed mutagenesis [42]. We modeled the structure of hAS3MT (Fig. 10) through 3D-JIGSAW Comparative Modelling Server. In the model, the active-site Cys residue was surface-exposed and was consistent with that in the mouse AS3MT model reported by Fomenko [59]. There are two Asn residues (Asn155 and Asn159) and one Ser resiude (Ser154) around Cys156 while one Trp residue (Trp203) and one Glu residue (Glu205) around Cys206. These residues all have electron-rich groups (amide group for Asn, hydroxy group for Ser, indole ring for Trp, and carboxyl group for Glu) and tend to coordinate with metal ions. Considering the high affinity of Co^{2+}, Mn^{2+} and Zn^{2+} for S, O, and N and integrating the inhibition manners (mixed manner for Co^{2+}, Mn^{2+} and competitive manner for Zn^{2+}) and the data from the DTNB assay, we conjecture that Co^{2+} and Mn^{2+} might coordinate with some of the electron-rich group residues, such as Asn155, Asn 159, Ser154, Trp203, and Glu205, as well as one or two of the active sites (Cys156 and Cys206) and/or other Cys residues while Zn^{2+} acted on all the active sites (Cys156 and Cys206) and other nearby residues. When metal ions combined with hAS3MT, the conformation of hAS3MT changed and the activity decreased. According to the DTNB data, Fe^{2+} also acted on the Cys residues of hAS3MT. However, it affected the activity of hAS3MT only in a very high concentration. This may attribute to that Fe^{2+} first acts on the Cys residues which are not contributory to the structure maintenance and the activity of hAS3MT.

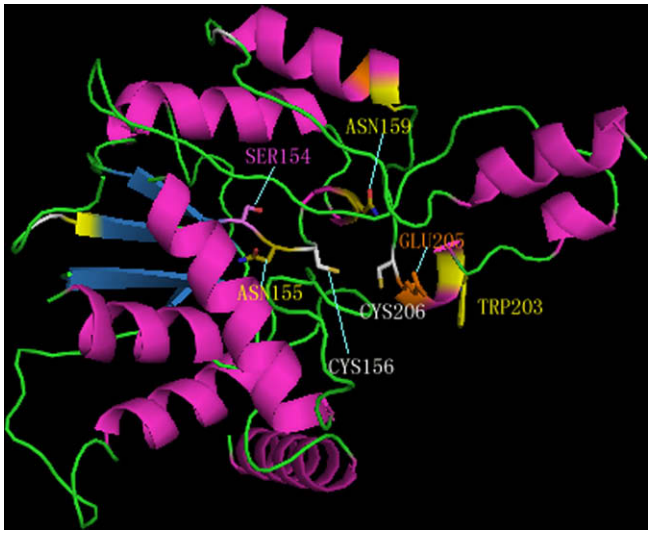

Fig. 10. 3D structural model of hAS3MT through 3D-JIGSAW Comparative Modelling Server. The residues are shown as stick model.

A 24 h dialysis of the hAS3MT–M^{2+}/SeO_3^{2-} (enzyme-inhibitors) against 25 mM PBS (pH 7.0) at 4 °C partially reversed the inhibition of hAS3MT activity by Co^{2+} and Mn^{2+} while that by Zn^{2+} or SeO_3^{2-} was almost totally reversed. CD spectra monitored that the secondary structure of hAS3MT–Zn^{2+}/SeO_3^{2-} enzyme was consistent with that of hAS3MT [22] after a 24 h dialysis at 4 °C. However, the conformation of hAS3MT–Co^{2+}/Mn^{2+} enzyme could not be totally reversed (Table 1) although there were no metal ions left in the enzyme solutions after the dialysis. These results also illuminated that Co^{2+} and Mn^{2+} acted on hAS3MT in different manners as compared with Zn^{2+} and SeO_3^{2-}.

Previous studies have suggested that there are four different types of reactions by which selenite might modify proteins: (a) formation of bis (S-cysteinyl) selenide (selenotrisulfide) bonds (–S–Se–S–); (b) catalysis of disulfide bonds formation (–S–S–); (c) formation of S-selanylcysteine, selenoylsulfide bonds (–S–Se–); (d) catalysis of disulfide bonds rupture [60]. Gather proposed that selenium toxicity was attributed to its interactions with proteins to form bis (S-cysteinyl) selenide, (RS-Se-SR) [61]. The inhibition of rat brain prostaglandin-D synthetase by selenite was suggested as a selenotrisulfide bond type. This inhibition was reversed by an excess DTT [62]. The inhibitory action of selenite on Caspase-3 was also affected by DTT not GSH, suggesting formation of a selenotrisulfide or disulfide [63]. Our data showed that the inhibition of hAS3MT activity by SeO_3^{2-} was substantially reversed by incubation with 2 mM DTT but not with 10 mM cysteine or 10 mM β-ME (Fig. 9A). These results demonstrated that the inhibitory effect of selenite on hAS3MT activity might be via formation of RS-Se-SR adducts with protein thiols or disulfide and further enriched the previous report [22,61]. For the inhibition by Co^{2+}, Mn^{2+}, and Zn^{2+}, 10 mM cysteine but not 10 mM β-ME reversed it. This may attribute to that high concentration cysteine will compete with hAS3MT to coordinate with the metal ions to release the ions from hAS3MT. However, β-ME is unaccessible to be close to the enzyme hydrophobic center or region to release the metal ions since it has a hydrophilic group, hydroxy. In addition, 2 mM DTT could also reverse the inhibition, suggesting a disulfide type or a RS-metal-SR

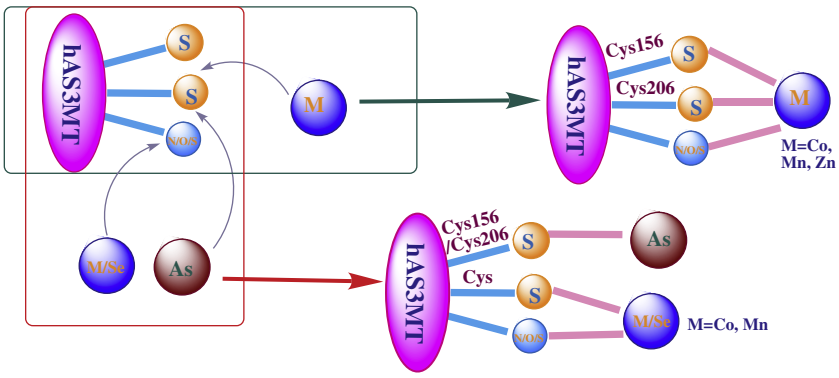

Scheme 1. Possible interaction modes of transition metal ions/selenite with hAS3MT. M = metal (Co, Mn, Zn).

type might be also involved in the inhibitory action on hAS3MT by Co^{2+}, Mn^{2+}, and Zn^{2+}. Integrating the data that the conformation of hAS3MT–Co^{2+}/Mn^{2+} enzyme could not be totally reversed (Table 1) after the dialysis, Co^{2+} and Mn^{2+}, in addition to the RS-Co/Mn-SR type, probably also catalyzed a disulfide formation in the enzyme by which they inhibited the activity of hAS3MT. For Zn^{2+} and SeO_3^{2-}, a RS-Zn/Se-SR type was probably used when they inhibited the activity of hAS3MT. According to our findings above, the possible path for the inhibition by transition metal ions and selenite through their interactions with hAS3MT might be estimated in Scheme 1.

In summary, This report demonstrates transition metal ions and selenite modulate the iAs^{3+} methylation by hAS3MT in vitro. They modify the structure and activity of hAS3MT through their interactions with the enzyme. Kinetic experiments showed that Co^{2+} and Mn^{2+} to be mixed (competitive and non-competitive) inhibitors of iAs^{3+} methylation by hAS3MT while Zn^{2+} to be a competitive inhibitor. The inhibitory effect of SeO_3^{2-} and Zn^{2+} on hAS3MT activity was almost via a RS-Zn/Se-SR type. For the inhibition by Co^{2+} and Mn^{2+}, in addition to the disulfide type, perhaps RS-Co/Mn-SR type was also used. However, some uncertainties about the inhibition mechanisms of transition metal ions and selenite as well as the impacts of transition metals on the iAs^{3+} methylation in vivo should be further studied.

5. Abbreviations

iAs	inorganic arsenic
MMA^{5+}	monomethylarsonic acid
DMA^{5+}	dimethylarsinic acid
AS3MT	arsenic(+3) methyltransferase
IPTG	isopropyl β-D-thiogalactopyranoside
BSA	bovine serum albumin
SAM	S-adenosyl-methionine
DTNB	5,5′-dithiobis (2-nitrobenzoic acid)
β-ME	β-mercaptoethanol
ICP-MS	inductively coupled plasma mass spectrometry
ROS	reactive oxygen species
M^{2+}	divalent transition metal ions (Co^{2+}, Mn^{2+}, Zn^{2+}, Fe^{2+})
PBS	phosphate-buffered saline

Acknowledgments

This work is supported by the National Natural Science Foundation of China (20535020, 20671051, 20721002 and 90813020), the National Basic Research Program of China (2007CB925102), and the Key Research Program of Ministry of Education of China (105081).

References

[1] D.J. Thomas, M. Styblo, S. Lin, Toxicol. Appl. Pharmacol. 176 (2001) 127–144.
[2] H.V. Aposhian, B. Zheng, M.M. Aposhian, X.C. Le, M.E. Cebrian, W. Cullen, R.A. Zakharyan, M. Ma, R.C. Dart, Z. Cheng, P. Andrews, L. Yip, G.F. O'Malley, R.M. Maiorino, W. Van Voorhies, S.M. Healy, A. Titcomb, Toxicol. Appl. Pharmacol. 165 (2000) 74–83.
[3] X.C. Le, M. Ma, X. Lu, W.R. Cullen, H.V. Aposhian, B. Zheng, Environ. Health Perspect. 108 (2000) 1015–1018.
[4] C.O. Abernathy, D.J. Thomas, R.L. Calderon, J. Nutr. 133 (2003) 1536S–1538S.
[5] T.G. Rossman, Mutat. Res. 533 (2003) 37–65.
[6] M.P. Waalkes, J. Liu, J.M. Ward, B.A. Diwan, Toxicology 198 (2004) 31–38.
[7] S. Nesnow, B.C. Roop, G. Lambert, M. Kadiiska, R.P. Mason, W.R. Cullen, M.J. Mass, Chem. Res. Toxicol. 15 (2002) 1627–1634.
[8] J.P. Buchet, R. Lauwerys, H. Roels, Int. Arch. Occup. Environ. Health 48 (1981) 71–79.
[9] S.K. Hirano, Y. Kobayashi, X. Cui, S. Kanno, T. Tayakawa, A. Shraim, Toxicol. Appl. Pharmacol. 198 (2004) 458–467.
[10] P.B. Tchounwou, J.A. Centeno, A.K. Patlolla, Mol. Cell Biochem. 255 (2004) 47–55.
[11] C.O. Abernathy, Y.P. Liu, D. Longfellow, H.V. Aposhian, B. Beck, B. Fowler, R. Goyer, R. Menzer, T. Rossman, C. Thompson, Environ. Health Perspect. 107 (1999) 593–597.
[12] C.X. Zhong, L. Wang, M.J. Mass, Toxicol. Lett. 122 (2001) 223–234.
[13] J. Popovicova, G.J. Moser, T.L. Goldsworthy, R.R. Tice, Toxicologist 54 (2000) 134.
[14] M. Styblo, D.J. Thomas, Toxicol. Appl. Pharmacol. 172 (2001) 52–61.
[15] O.A. Levander, Environ. Health Perspect. 19 (1977) 159–164.
[16] D. Ganyc, S. Talbot, F. Konate, S. Jackson, B. Schanen, W. Cullen, W.T. Self, Environ. Health Perspect. 115 (2007) 346–353.
[17] H. Babich, N. Martin-Alguacil, E. Borenfreund, Toxicol. Lett. 45 (1989) 157–164.
[18] F.S. Walton, S.B. Waters, S.L. Jolley, E.L. LeCluyse, D.J. Thomas, Chem. Res. Toxicol. 16 (2003) 261–265.
[19] Z. Gregus, A. Gyurasics, L. Koszorus, Environ. Toxicol. Pharmacol. 5 (1998) 89–99.
[20] W.J. Christian, C. Hopenhayn, J.A. Centeno, T. Todorov, Environ. Res. 100 (2006) 115–122.
[21] M. Styblo, M. Delnomdedieu, D.J. Thomas, Chem. Biol. Interact. 99 (1996) 147–164.
[22] Z.R. Geng, X.L. Song, Z. Xing, J.L. Geng, S.C. Zhang, X.R. Zhang, Z.L. Wang, J. Biol. Inorg. Chem. 14 (2009) 485–496.
[23] S.A. Manley, G.N. George, I.J. Pickering, R.S. Glass, E.J. Prenner, R. Yamdagni, Q. Wu, J. Gailer, Chem. Res. Toxicol. 19 (2006) 601–607.
[24] J. Gailer, G.N. George, I.J. Pickering, R.C. Prince, H.S. Younis, J.J. Winzerling, Chem. Res. Toxicol. 15 (2002) 1466–1471.
[25] J. Gailer, G.N. George, I.J. Pickering, R.C. Prince, S.C. Ringwald, J.E. Pemberton, R.S. Glass, H.S. Younis, D.W. DeYoung, H.V. Aposhian, J. Am. Chem. Soc. 122 (2000) 4637–4639.
[26] R. Bailly, R. Lauwerys, J.P. Buchet, P. Mahieu, J. Konings, Brit. J. Ind. Med. 48 (1991) 93–97.
[27] T. Gebel, Mutat. Res. 412 (1998) 213–218.
[28] P. Andrewes, W.R. Cullen, E. Polishchuk, Environ. Sci. Technol. 34 (2000) 2249–2253.
[29] K. Michalke, R. Hensel, in: A.V. Hirner, H. Emons (Eds.), Organic Metal and Metalloid Species in the Environment, Biovolatilisation of metal(loid)s by microorganisms, vol. 7, Springer-Verlag, New York, 2004, pp. 137–150.
[30] J.P. Buchet, R. Lauwerys, Arch. Toxicol. 57 (1985) 125–129.
[31] J.S. Thayer, Appl. Organometal. Chem. 16 (2002) 677–691.

[32] W.T. Frankenberger Jr., M. Arshad, in: W.T. Frankenberger Jr. (Ed.), Environmental Chemistry of Arsenic, vol. 16, Volatilization of Arsenic, Marcel Dekker Inc., New York, 2002, pp. 363–380.
[33] J.D. Kimpe, R. Cornelis, R. Vanholder, Drug Chem. Toxicol. 22 (1999) 613–628.
[34] T. Kuroki, T. Matsushima, Mutagenesis 2 (1987) 33–37.
[35] Y.T. Yang, C.S.C. Wu, H.M. Martinez, Methods Enzymol. 130 (1986) 208–257.
[36] J. Versieck, J.T. McCall, Crit. Rev. Clin. Lab. Sci. 22 (1985) 97–184.
[37] H. Naranmandura, N. Suzuki, K.T. Suzuki, Chem. Res. Toxicol. 19 (2006) 1010–1018.
[38] J. Gailer, S. Madden, W.R. Cullen, M.B. Denton, Appl. Organometal. Chem. 13 (1999) 837–843.
[39] G. Raber, K.A. Francesconi, K.J. Irgolic, W. Goessler, Fresenius J. Anal. Chem. 367 (2000) 181–188.
[40] Z. Šlejkovec, I. Falnoga, W. Goessler, J.T. van Elteren, R. Raml, H. Podgornik, P. Černelč, Anal. Chim. Acta 607 (2008) 83–91.
[41] G.L. Ellman, Arch. Biochem. Biophys. 82 (1959) 70–77.
[42] X.L. Song, Z.R. Geng, J.S. Zhu, C.Y. Li, X. Hu, N.S. Bian, X.R. Zhang, Z.L. Wang, Chem. Biol. Interact. 179 (2009) 321–328.
[43] R.A. Zakharyan, G. Tsaprailis, U.K. Chowdhury, A. Hernandez, H.V. Aposhian, Chem. Res. Toxicol. 18 (2005) 1287–1295.
[44] T.R. Chowdhury, G.K. Basu, B.K. Mandal, B.C. Raymahashay, S. Guha, A. Bhowmik, Nature 401 (1999) 545–547.
[45] E. Stokstad, Science 298 (2002) 1535–1537.
[46] W.R. Cullen, B.C. McBride, J. Reglinski, J. Inorg. Biochem. 21 (1984) 45–60.
[47] E.A. Crecelius, Environ. Health Perspect. 19 (1977) 147–150.
[48] D.J. Thomas, S.B. Waters, M. Styblo, Toxicol. Appl. Pharmacol. 198 (2004) 319–326.
[49] R.W.J. Sarver, W.C. Krueger, Anal. Biochem. 199 (1991) 61–67.
[50] J.P. Hennessey, W.C. Johnson, Biochemistry 20 (1981) 1085–1094.
[51] P. Manavalan, W.C. Johnson, Proc. Int. Sympos. Biomol. Struct. Interact, Suppl. J. Biosci. 8 (1985) 141–149.
[52] Y. Chen, M.D. Barkley, Biochemistry 37 (1998) 9976–9982.
[53] T. Gensch, J. Hendriks, K.J. Hellingwerf, Photochem. Photobiol. Sci. 3 (2004) 531–536.
[54] J.T. Vivian, P.R. Callis, Biophys. J. 80 (2001) 2093–2109.
[55] W.C. Lam, D.H.H. Tsao, A.H. Maki, K.A. Maegley, N.O. Reich, Biochemistry 31 (1992) 10438–10442.
[56] E.P. Painter, Chem. Rev. 28 (1941) 179–213.
[57] H.E. Ganther, Biochemistry 7 (1968) 2898–2905.
[58] A. Terada, M. Yoshida, Y. Seko, T. Kobayashi, K. Yoshida, M. Nakada, K. Nakada, H. Echizen, H. Ogata, T. Rikihisa, Nutrition 15 (1999) 651–655.
[59] D.E. Fomenko, W.B. Xing, B.M. Adair, D.J. Thomas, V.N. Gladyshev, Science 315 (2007) 387–389.
[60] M. Birringer, S. Pilawa, L. Flohe, Nat. Prod. Rep. 19 (2002) 693–718.
[61] H.E. Ganther, Carcinogenesis 20 (1999) 1657–1666.
[62] F. Islam, Y. Watanabe, H. Morii, O. Hayaishi, Arch. Biochem. Biophys. 289 (1991) 161–166.
[63] H.S. Park, S.U. Huh, Y. Kim, J. Shim, S.H. Lee, S. Park, Y.K. ung, I.Y. Kim, E.J. Choi, J. Biol. Chem. 275 (2000) 8487–8491.